Chemical Engineering Journal 163 (2010) 154–159

Contents lists available at ScienceDirect

Chemical Engineering Journal

journal homepage: www.elsevier.com/locate/cej

Synthesis and properties of microencapsulated paraffin composites with SiO_2 shell as thermal energy storage materials

Guiyin Fang[a,*], Zhi Chen[a], Hui Li[b]

[a] School of Physics, Nanjing University, Hankou Road 22, Nanjing 210093, Jiangsu, China
[b] Department of Material Science and Engineering, Nanjing University, Nanjing 210093, China

ARTICLE INFO

Article history:
Received 15 June 2010
Received in revised form 17 July 2010
Accepted 22 July 2010

Keywords:
Composites
Microencapsulated phase change material
Sol–gel
Thermal properties
Thermal energy storage

ABSTRACT

Microencapsulated paraffin composites with SiO_2 shell as thermal energy storage materials were prepared using sol–gel methods. In the microencapsulated composites, paraffin was used as the core material that is a phase change material (PCM), and SiO_2 acted as the shell material that is fire resistant. Fourier transformation infrared spectroscope (FT-IR), X-ray diffractometer (XRD) and scanning electronic microscope (SEM) were used to determine chemical structure, crystalloid phase and microstructure of microencapsulated paraffin composites with SiO_2 shell, respectively. The thermal properties were investigated by a differential scanning calorimeter (DSC). The thermal stability was determined by a thermogravimetric analyzer (TGA). The SEM results showed that the paraffin was well encapsulated in the shell of SiO_2. The DSC results indicated that the microencapsulated paraffin composites solidify at 58.27 °C with a latent heat of 107.05 kJ/kg and melt at 58.37 °C with a latent heat of 165.68 kJ/kg when the encapsulation ratio of the paraffin is 87.5%. The TGA results showed that the SiO_2 shells can improve the thermal stability of the microencapsulated paraffin composites due to the synergistic effect between the paraffin and SiO_2.

1. Introduction

Phase change materials (PCMs) have received attention in solar heating system [1,2], building energy conservation [3,4] and air-conditioning systems [5,6]. PCMs are developed for various applications due to their different phase change intervals: materials that melt below 15 °C are used for keeping coolness in air-conditioning applications, while materials that melt above 90 °C are used to drop the temperature if there is a sudden increase in heat to avoid ignition. All other materials that melt between these two temperatures can be applied in solar heating and building energy conservation systems. Many inorganic and organic PCMs (salt hydrates, paraffins, fatty acids/esters, etc.) and PCM mixtures have been studied for latent heat storage application [7,8]. Among the PCMs investigated, paraffins have been widely used due to their high latent heat storage capacity and appropriate thermal properties, such as little or no supercooling, low vapor pressure, good thermal and chemical stability, and self-nucleating behavior [9]. However, they have low thermal conductivity, and need encapsulation in order to prevent leakage of the melted PCM during the phase change process [10]. Now, these problems can be solved by using microencapsulated PCMs. Microencapsulated PCMs (MEPCMs) can greatly increase the heat transfer efficient, enlarge the heat transfer area, reduce PCM reactivity towards the outside environment and control the changes in the volume as phase change occurs [11,12]. Various methods have been developed for the encapsulation of PCMs, such as complex coacervation [13], interfacial polycondensation [14] and *in situ* polymerization [15].

A typical microencapsulation process is the one which uses formaldehyde resins for the protection of PCMs, like melamine–formaldehyde resins [16–18] and urea–formaldehyde resins [19–21]. However, melamine–formaldehyde and urea–formaldehyde resins shell materials usually release poisonous formaldehyde in the application, which can cause environmental and health problems. In addition, due to the chemical constitution of organic PCMs (paraffins, fatty acids/esters, etc.) and organic polymer shell materials, the microencapsulated PCMs are easily flammable, and their application is therefore severely restricted [22].

In this paper, the synthesis and properties of microencapsulated paraffin composites with SiO_2 shell are reported. In the microencapsulated composites, paraffin was used as the latent heat storage material, and SiO_2 served as the inorganic shell material. The paraffin is a favorable organic PCM for thermal energy storage, melting at 59.26 °C with a latent heat of 189.24 kJ/kg and solidifying at 54.75 °C with a latent heat of 193.73 kJ/kg (experimental data of the paraffin in Table 2). SiO_2 is an inorganic amorphous material that is fire resistant [23,24].

* Corresponding author. Tel.: +86 25 51788228; fax: +86 25 83593707.
E-mail address: gyfang@nju.edu.cn (G. Fang).

1385-8947/$ – see front matter © 2010 Elsevier B.V. All rights reserved.
doi:10.1016/j.cej.2010.07.054

Table 1
The compositions of the paraffin and SDS in the oil/water emulsion.

Samples	Compositions
MEPCM1	10 g paraffin + 100 ml distilled water + 0.2 g SDS
MEPCM2	15 g paraffin + 150 ml distilled water + 0.3 g SDS
MEPCM3	20 g paraffin + 200 ml distilled water + 0.4 g SDS

It is known from the above literatures that the encapsulation method of PCMs by sol–gel process is little reported. In addition, because organic PCMs (paraffin, etc.) with organic polymer shell materials have flammability, they are not widely applied in thermal energy storage system. In this research, the SiO_2 shells can improve the thermal stability and flammability of the microencapsulated paraffin composites due to the synergistic effect between the paraffin and SiO_2. Therefore, the latent heat of microencapsulated paraffin composites with SiO_2 shell can be utilized for thermal energy storage in solar heating and building energy conservation systems.

2. Experimental

2.1. Materials

Tetraethyl silicate (Reagent grade, Sinopharm Chemical Reagent Company) was used as the precursor. Anhydrous ethanol (Reagent grade, Nanjing Chemical Reagent Company) and distilled water acted as solvent. Hydrochloric acid (Reagent grade, Nanjing Chemical Reagent Company) was used as the activator. Paraffin (Reagent grade, Nanjing Huakang Chemical Reagent Company) was used as latent heat storage PCM. The paraffin is saturated alkanes (C_nH_{2n+2}) with melting point of 56–60 °C, melting latent heat of 189.24 kJ/kg, specific heat of 1.93 kJ/kg °C and density of 916 kg/m^3. Sodium dodecyl sulfate (SDS) (Reagent grade, Shanghai Chemical Reagent Company) was used as oil–water emulsifier.

2.2. Preparation of paraffin O/W emulsion

In one beaker, SDS was dissolved in distilled water. Then, paraffin was added into this solution and continuously stirred at a rate of 1000 rpm for 2 h with a magnetic stirrer while the temperature of the solution was controlled at 70 °C using a constant temperature bath. In order to form a stable oil/water emulsion and obtain a better performance of microencapsulated paraffin composites, different amounts of paraffin and SDS were chosen during preparation process. The compositions of the paraffin and SDS in the oil/water emulsion are listed in Table 1. Finally, the paraffin was uniformly dispersed in an aqueous solution containing SDS emulsifier to form a stable O/W microemulsion.

2.3. Preparation of microencapsulated paraffin composites with SiO_2 shell

20 g tetraethyl silicate, 20 g anhydrous ethanol and 40 g distilled water were added to another beaker. The pH of the mixture was adjusted to 2–3 by adding a little hydrochloric acid, the mixture was stirred at a rate of 500 rpm for 30 min with a magnetic stirrer while the temperature of the mixture was controlled at 60 °C using a constant temperature bath. After the hydrolysis reaction of the tetraethyl silicate had taken place, the sol solution as encapsulation precursor was obtained. The hydrolysis reaction mechanism of the tetraethyl silicate is shown in Scheme 1.

$$Si(OC_2H_5)_4 + H_2O \longrightarrow Si(OH)_4 + C_2H_5OH$$

Scheme 1. The hydrolysis reaction mechanism of the tetraethyl silicate.

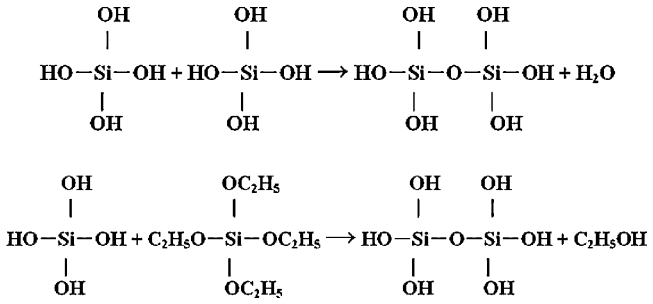

Scheme 2. The condensation reaction mechanism of the tetraethyl silicate.

The sol solution was added dropwise into the prepared paraffin O/W emulsion with stirring at a rate of 500 rpm for 4 h using a magnetic stirrer whilst the temperature of the sol solution was controlled at 70 °C using a constant temperature bath. The condensation reaction mechanism of the tetraethyl silicate onto the surface of paraffin droplet is shown in Scheme 2. In Scheme 2, the sol mixture was formed by condensation reactions of the silicic acid and silicic acid or the silicic acid and tetraethyl silicate. After the polymerization process of the sol mixture was completed, the SiO_2 shell was formed on the surface of paraffin droplet. The shell formation process of the SiO_2 is shown in Scheme 3. Finally, white powders were collected by filter paper at normal pressure and washed with distilled water. The microencapsulated composites were dried in a vacuum oven at 50 °C for 20 h. Three kinds of microencapsulated paraffin composites with SiO_2 shell were obtained after drying at 50 °C for 10 h, denoted MEPCM1, MEPCM2 and MEPCM3.

When the mass of distilled water in the solution increases, the hydrolysis process of the tetraethyl silicate can be promoted. However, the concentration of silicic acid may reduce, and the hydrolysis reaction of the silicic acid takes place again. This will prolong condensation reaction process of the tetraethyl silicate.

The hydrolysis reaction of the tetraethyl silicate is very slow at room temperature. In order to accelerate the hydrolysis process of the tetraethyl silicate, the temperature of the mixture was controlled at 60 °C using a constant temperature bath. When the pH of the mixture is 2–3, the sol solution is very steady. Therefore, the hydrochloric acid is added in the mixture to adjust the pH value of the solution.

2.4. Characterization of microencapsulated paraffin composites with SiO_2 shell

The morphology and microstructure of microencapsulated paraffin composites with SiO_2 shell were observed using a scanning electronic microscope (SEM, S-3400N II, Hitachi Inc., Japan). The structural analysis of the microencapsulated paraffin composites with SiO_2 shell was carried out using a FT-IR spectrophotometer. The FT-IR spectra were recorded on a Nicolet Nexus 870 from 400 to 4000 cm^{-1} with a resolution of 2 cm^{-1} using KBr pellets. The crystalloid phase of the microencapsulated paraffin was investigated by XRD (D/MAX-Ultima III, Rigaku Corporation, Japan). The XRD patterns were obtained with continuous scanning mode at the rate of 5° (2θ)/min and operating conditions of 40 kV and 40 mA. The thermal properties of the microencapsulated paraffin composites with SiO_2 shell were measured using a differential scanning calorimeter (Pyris 1 DSC, Perkin-Elmer) at 5 °C/min under a constant stream of argon at a flow rate of 20 ml/min. The accuracy of

$$n\ (Si-O-Si) \longrightarrow (-Si-O-Si-)_n$$

Scheme 3. The shell formation process of the SiO_2.

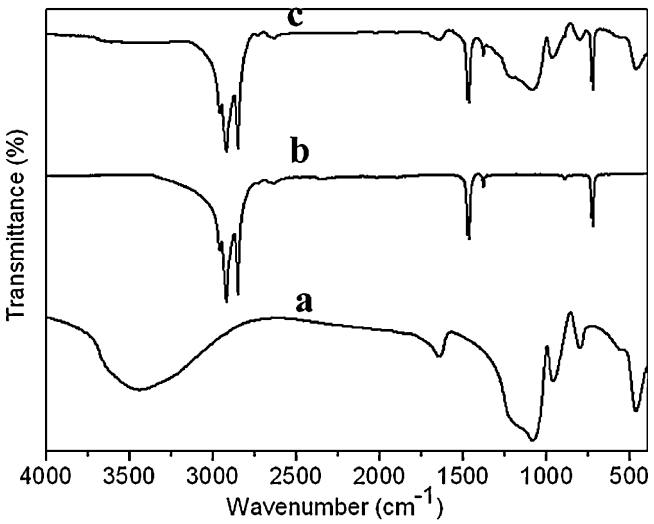

Fig. 1. FT-IR spectra of the (a) SiO_2, (b) paraffin and (c) MEPCM3.

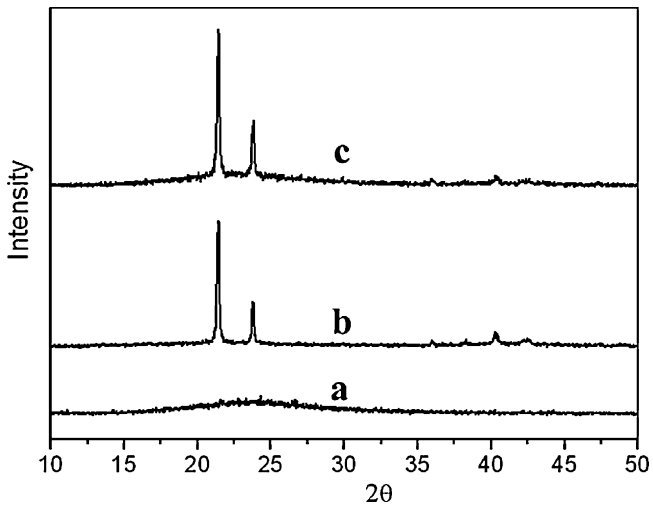

Fig. 2. XRD patterns of the (a) SiO_2, (b) paraffin and (c) MEPCM3.

enthalpy measurements was ±5% and the temperature accuracy was ±0.2 °C. Three measurements were done for each sample and mean enthalpy value was regarded as latent heat of the microencapsulated paraffin with maximum random error of ±6 kJ/kg. The thermal stability of the microencapsulated paraffin composites with SiO_2 shell was determined by a thermogravimetric analyzer (Pyris 1 TGA, Perkin-Elmer) from room temperature to 700 °C with a linear heating rate of 20 °C/min under a constant stream of nitrogen at a flow rate of 20 ml/min.

3. Results and discussion

3.1. FT-IR analysis of microencapsulated paraffin composites with SiO_2 shell

The FT-IR spectra of the MEPCM1 and MEPCM2 are the same as that of the MEPCM3 due to they contain the same kind of materials. So the FT-IR spectra of the MEPCM3 were chosen for the FT-IR analysis. The FT-IR spectra of the SiO_2, paraffin and MEPCM3 are shown in Fig. 1. Fig. 1a shows the spectrum of the SiO_2. The peaks at 1083, 798 and 463 cm^{-1} signify the bending vibration of the Si–O functional group and the peak at 960 cm^{-1} is assigned to the Si–OH functional group. The absorption bands at 3000–3600 cm^{-1} and 1600–1700 cm^{-1} represent the stretching and bending vibrations of the–OH functional group of H_2O. Fig. 1b shows the spectrum of the paraffin. The peak at 2917 cm^{-1} signifies the symmetrical stretching vibration of its $-CH_3$ group, the peak at 2849 cm^{-1} represents the symmetrical stretching vibration of its–CH_2 group. The peaks at around 1463 cm^{-1} belong to the deformation vibration of–CH_2 and–CH_3, and the peak at 719 cm^{-1} represents the rocking vibration of $-CH_2$.

As shown in Fig. 1c, the absorption peaks of the SiO_2 at 1083, 960, 798 and 463 cm^{-1} also appear in the MEPCM3 spectra. Due to the SiO_2 can only be formed on the interface of paraffin O/W emulsion, the FT-IR results indicate that the SiO_2 shell was formed on the surface of paraffin droplet. The absorption peaks of the paraffin at 2917, 2849, 1463 and 719 cm^{-1} are not changed in the MEPCM3 spectra. This result indicates that there is no chemical interaction between the paraffin molecule and SiO_2. The paraffin was encapsulated easily in the shells of the SiO_2 through the condensation and polymerization process of the obtained SiO_2 precursors from the hydrolysis of the tetraethyl silicate.

3.2. XRD patterns of microencapsulated paraffin composites with SiO_2 shell

The XRD patterns of the SiO_2, paraffin and MEPCM3 are presented in Fig. 2. Fig. 2a shows that SiO_2 has a flat peak at around 25°. This result indicates that the SiO_2 is non-crystalline with amorphous structure so that the SiO_2 shell can be completely formed. As shown in Fig. 2b, the XRD peaks at 21.5° and 23.8° are caused by the paraffin due to its regular crystallization. It can be found in Fig. 2c that the XRD peaks of the paraffin in the microencapsulated composites are also presented on basis of the SiO_2 flat peak. Because the SiO_2 cannot be formed within the paraffin droplet, this result also indicates that the paraffin was encapsulated in the SiO_2 shells.

3.3. Morphology of microencapsulated paraffin composites with SiO_2 shell

Fig. 3 shows SEM photographs of the MEPCM1, MEPCM2 and MEPCM3. As shown in Fig. 3, the paraffin was encapsulated in the shells of the SiO_2. The SiO_2 shells provided the mechanical strength for the microencapsulated composites and prevented the seepage of the melted paraffin. It is also observed from Fig. 3a–f that morphologies of the MEPCM2 and MEPCM3 are more homogeneous than that of the MEPCM1. This is because the mass of the paraffin in the MEPCM1 is smaller than that in the MEPCM2 and MEPCM3, which results in the SiO_2 shells were not well formed on the surface of the paraffin droplet due to the conglomeration of the SiO_2. We also know from Fig. 3 that the size distribution of the MEPCM is uniform and the size of the MEPCM is about 8–15 μm.

3.4. Thermal properties of microencapsulated paraffin composites with SiO_2 shell

The DSC results of the paraffin, MEPCM1, MEPCM2 and MEPCM3 are presented in Figs. 4 and 5; Table 2. There are two absorbing heat peaks in Fig. 4, the small peak represents solid–solid transition process and the big peak denotes solid–liquid melting process. Before the melting, the solid–solid transition is induced by phase transformation from an ordered phase to a more disordered rotator phase. As shown in Fig. 5, the big peak and small peak denote liquid–solid solidification process and solid–solid transition process, respectively. In Figs. 4 and 5, solid–liquid melting peak and liquid–solid solidification peak were used to calculate the melting and solidifying latent heat value.

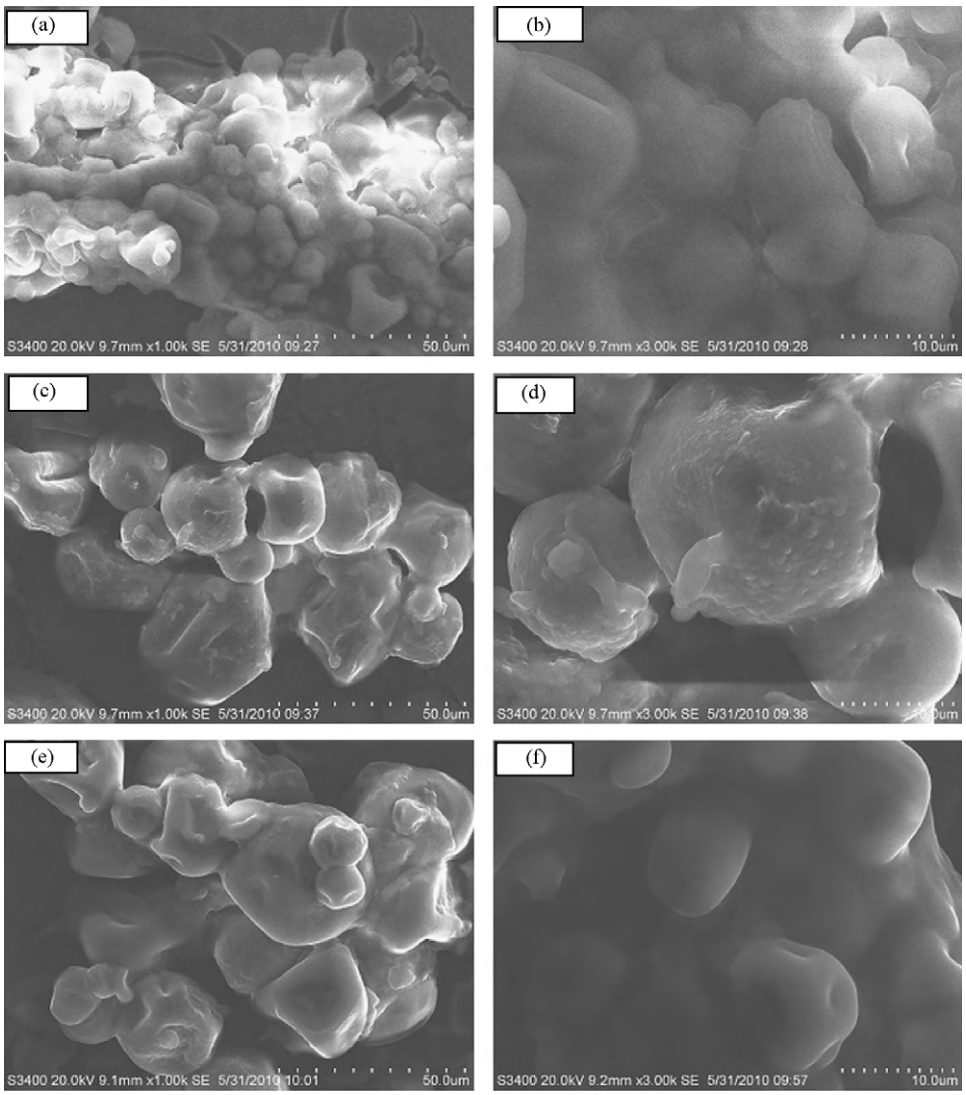

Fig. 3. SEM photographs of the (a) MEPCM1 (1k×), (b) MEPCM1 (3k×), (c) MEPCM2 (1k×), (d) MEPCM2 (3k×), (e) MEPCM3 (1k×) and (f) MEPCM3 (3k×).

Comparing the latent heat data of the microencapsulated composites with those of the paraffin, the encapsulation ratio of the paraffin can be determined from Eq. (1). The value of η is the encapsulation ratio of the paraffin in the composites, ΔH_{MEPCM} represents the melting latent heat of the microencapsulated composites, and ΔH_{PCM} represents the melting latent heat of the paraffin as measured by the DSC.

$$\eta\% = \frac{\Delta H_{MEPCM}}{\Delta H_{PCM}} \times 100 \quad (1)$$

The encapsulation ratio of the paraffin in the composites was calculated and the values are also presented in Table 2. It is known that the encapsulation ratio of the paraffin in the MEPCM3 is larger than that in the MEPCM1 and MEPCM2.

As shown in Table 2, the melting and solidifying temperatures are measured to be 59.26 and 54.75 °C for the paraffin, and to be 58.37 and 57.02 °C for the MEPCM3. The phase change characteristics of the microencapsulated composites are close to those of the paraffin. It is also known from Table 2 that the melting and solidifying latent heats are measured to be 189.24 and 193.73 kJ/kg for the paraffin, and to be 165.68 and 107.65 kJ/kg for the MEPCM3. In the microencapsulated composites, high PCM content will result in a high latent heat storage capacity. Therefore, the MEPCM3 is chosen as a promising thermal energy storage material.

In Table 2, the melting latent heat of MEPCM is larger than the solidifying latent heat of MEPCM. This is due to fact that mass loss of MEPCM increases when the sample is heated from 10 to 100 °C during melting process test by the DSC. Thereafter, the solidify-

Table 2
DSC data of the paraffin, MEPCM1, MEPCM2 and MEPCM3.

Sample name	Encapsulation ratio of the paraffin (%)	Melting		Solidifying	
		Temperature (°C)	Latent heat (kJ/kg)	Temperature (°C)	Latent heat (kJ/kg)
Paraffin	100.0	59.26	189.24	54.75	−193.73
MEPCM1	69.1	57.84	130.82	57.01	−93.04
MEPCM2	77.6	57.68	146.80	56.73	−100.83
MEPCM3	87.5	58.37	165.68	57.02	−107.05

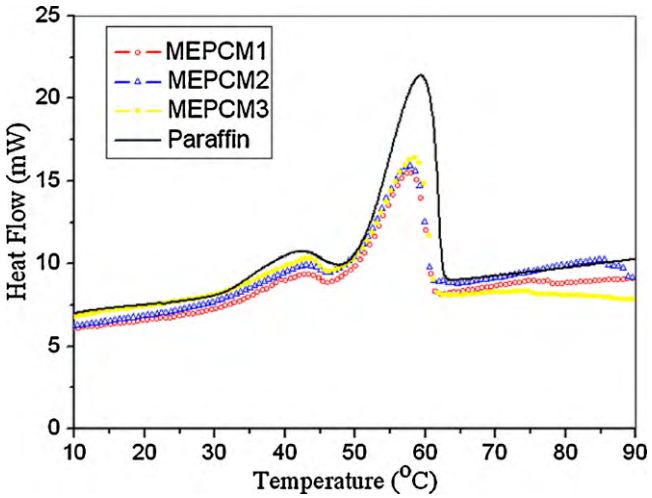

Fig. 4. The melting DSC curves of the paraffin, MEPCM1, MEPCM2 and MEPCM3.

ing process test of MEPCM is carried out. Because of mass loss of MEPCM in the melting process test, the solidifying latent heat of MEPCM is smaller than the melting latent heat of MEPCM in the solidifying process test.

The DSC results in Table 2 show that the melting and solidifying temperatures of the microencapsulated composites decrease by 0.25–1.8 °C when compared with the melting and solidifying temperatures of pure paraffin. This is due to the fact that there are no strong interactions between the paraffin molecules and the shells of the SiO_2. This leads to a depression of the phase change temperatures of the paraffin in the microencapsulated composites [25]. It is also known from Fig. 5 that the difference between solidifying onset temperature and peak temperature of the MEPCM1, MEPCM2 and MEPCM3 is smaller than that of the paraffin. This indicates the supercooling degree of the MEPCM1, MEPCM2 and MEPCM3 is smaller than that of the paraffin during solidification process due to interior wall of the SiO_2 shells could act as nucleation agent.

3.5. Thermal stability of microencapsulated paraffin composites with SiO_2 shell

The TGA and DTG curves of the MEPCM1, MEPCM2 and MEPCM3 are shown in Figs. 6 and 7. The charred residue amount at 700 °C and the temperature of maximum weight loss are presented in Table 3. It can be known from Fig. 6 that there are two-step thermal

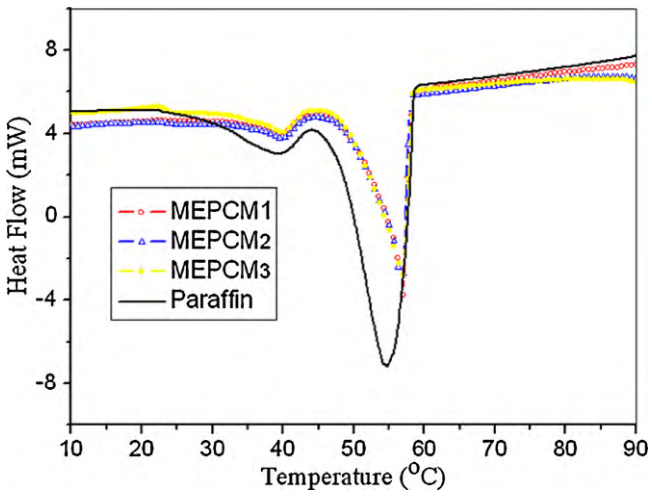

Fig. 5. The solidifying DSC curves of the paraffin, MEPCM1, MEPCM2 and MEPCM3.

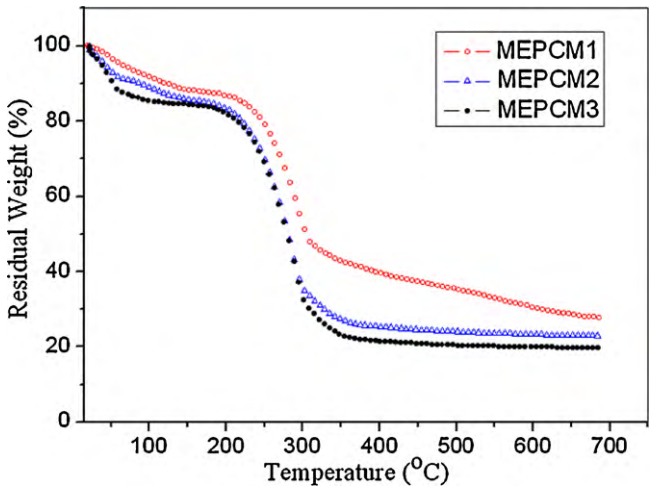

Fig. 6. TGA curves of the MEPCM1, MEPCM2 and MEPCM3.

Table 3
TGA data of the MEPCM1, MEPCM2 and MEPCM3.

Samples	T_1 (°C)	T_2 (°C)	Charred residue amount (%) (700 °C)
MEPCM1	45.7	288.6	27.61
MEPCM2	45.4	287.3	22.87
MEPCM3	50.9	292.1	19.65

degradation processes. The weight loss of the MEPCM3 is relatively larger than that of the MEPCM1 and MEPCM2 during two-step thermal degradation processes. This is because that the mass of the paraffin in the MEPCM3 is larger than that in the MEPCM1 and MEPCM2. As shown in Fig. 7, the first step occurs at the temperature between 20 and 80 °C, corresponding to the release of water molecules adsorbed in the shells of the SiO_2. The second step takes place from 200 to 350 °C, corresponding to the thermal degradation of the paraffin molecular chains. The TGA test of paraffin has been carried out by Song et al. [26]. Their results indicate that the thermal degradation of the paraffin molecular chains was between 200 and 400 °C, which accords with well the thermal degradation temperature of the paraffin in this MEPCM.

The weight loss of MEPCM3 obtained from the TGA result at the temperature between 20 and 80 °C is relatively larger than that in the MEPCM1 and MEPCM2. This is because the release of paraffin

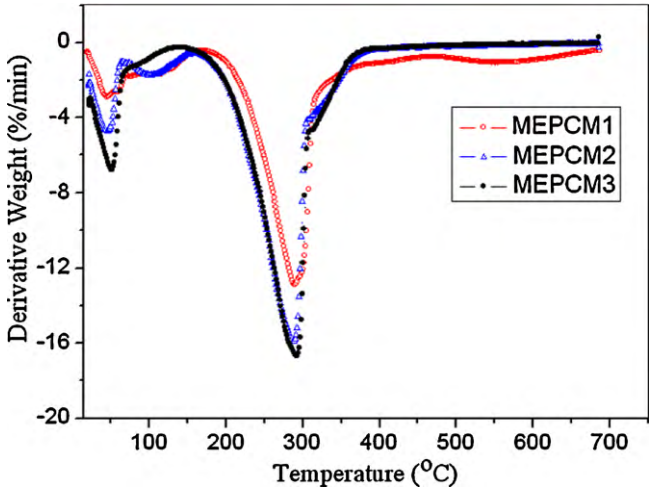

Fig. 7. DTG curves of the MEPCM1, MEPCM2 and MEPCM3.

molecules in the MEPCM3 is easier than that in the MEPCM1 and MEPCM2 due to the SiO_2 mass in the MEPCM3 is smaller than that in the MEPCM1 and MEPCM2.

As shown in Table 3, the onset temperatures (T_1) of the weight loss of the MEPCM3 is higher than that of the MEPCM1 and MEPCM2, the maximum temperatures (T_2) of the weight loss of the MEPCM3 are 3–5 °C higher than that of the MEPCM1 and MEPCM2. The charred residue amount of the MEPCM3 is smaller than that of the MEPCM1 and MEPCM2. It is because that the mass of the SiO_2 shells in the MEPCM3 is smaller than that in the MEPCM1 and MEPCM2. The SiO_2 shells are advantageous to form carbonaceous-silicate charred layer building up on the surface, which insulates the core material and slows the escape of the volatile products generated during thermal degradation. The carbonaceous-silicate charred layers may create a physical protective barrier on the surface of the microencapsulated composites. This protective barrier can limit the transfer of flammable molecules to the gas phase, the transfer of heat from the flame to the condensed phase and oxygen diffusion in the condensed phase [27]. This means that the SiO_2 shells can improve the thermal stability and flammability of the microencapsulated paraffin composites due to the synergistic effect between the paraffin and SiO_2.

4. Conclusions

The synthesis and properties of microencapsulated paraffin composites with SiO_2 shell are reported. The paraffin was used as the core material for thermal energy storage, and SiO_2 acted as the shell material for improving the thermal stability and flammability of the microencapsulated paraffin composites. The paraffin was well encapsulated in the shells of the SiO_2, and the leakage of melted paraffin from the microencapsulated composites can be prevented even when it was heated above the melting temperature of the paraffin. As the encapsulation ratio of the paraffin is 87.5%, the microencapsulated paraffin composites solidify at 58.27 °C with a latent heat of 107.05 kJ/kg and melt at 58.37 °C with a latent heat of 165.68 kJ/kg. The SiO_2 shells can improve the thermal stability of the microencapsulated paraffin composites due to the synergistic effect between the paraffin and SiO_2.

Acknowledgements

The authors thank the National Natural Science Foundation of China (Grant no. 50776043) for financial support of this research. The authors also wish to thank reviewers for kindly giving revising suggestions.

References

[1] B. Zalba, J.M. Marin, L.F. Cabeza, H. Mehling, Review on thermal energy storage with phase change: materials, heat transfer analysis and applications, Appl. Therm. Eng. 23 (2003) 251–283.
[2] W. Saman, F. Bruno, E. Halawa, Thermal performance of PCM thermal storage unit for a roof integrated solar heating system, Sol. Energy 78 (2005) 341–349.
[3] A.M. Khudhair, M.M. Farid, A review on energy conservation in building applications with thermal storage by latent heat using phase change materials, Energy Convers. Manage. 45 (2004) 263–275.
[4] F. Kuznik, J. Virgone, J. Noel, Optimization of a phase change material wallboard for building use, Appl. Therm. Eng. 28 (2008) 1291–1298.
[5] B.M. Diaconu, S. Varga, A.C. Oliveira, Experimental assessment of heat storage properties and heat transfer characteristics of a phase change material slurry for air conditioning applications, Appl. Energy 87 (2010) 620–628.
[6] F.Q. Wang, G. Maidment, J. Missenden, R. Tozer, The novel use of phase change materials in refrigeration plant. Part 3. PCM for control and energy savings, Appl. Therm. Eng. 27 (2007) 2911–2918.
[7] A. Sharma, V.V. Tyagi, C.R. Chen, D. Buddhi, Review on thermal energy storage with phase change materials and applications, Renew. Sustainable Energy Rev. 13 (2009) 318–345.
[8] R. Baetens, B.P. Jelle, A. Gustavsen, Phase change materials for building applications: a state-of-the-art review, Energy Build. 42 (2010) 1361–1368.
[9] B. He, V. Martin, F. Setterwall, Phase transition temperature ranges and storage density of paraffin wax phase change materials, Energy 29 (2004) 1785–1804.
[10] A. Sari, Form-stable paraffin/high density polyethylene composites as solid–liquid phase change material for thermal energy storage: preparation and thermal properties, Energy Convers. Manage. 45 (2004) 2033–2042.
[11] M.N.A. Hawlader, M.S. Uddin, M.M. Khin, Microencapsulated PCM thermal-energy storage system, Appl. Energy 74 (2003) 195–202.
[12] Y.M. Xuan, Y. Huang, Q. Li, Experimental investigation on thermal conductivity and specific heat capacity of magnetic microencapsulated phase change material suspension, Chem. Phys. Lett. 479 (2009) 264–269.
[13] Y. Rong, H.Z. Chen, D.C. Wei, J.Z. Sun, M. Wang, Microcapsules with compact membrane structure from gelatin and styrene–maleic anhydride copolymer by complex coacervation, Colloids Surf. A: Physicochem. Eng. Aspects 242 (2004) 17–20.
[14] K. Hong, S. Park, Preparation of polyurea microcapsules with different composition ratios: structures and thermal properties, Mater. Sci. Eng. A 272 (1999) 418–421.
[15] X.X. Zhang, Y.F. Fan, X.M. Tao, K.L. Yick, Fabrication and properties of microcapsules and nanocapsules containing *n*-octadecane, Mater. Chem. Phys. 88 (2004) 300–307.
[16] J. Su, L. Wang, L. Ren, Fabrication and thermal properties of microPCMs: used melamine–formaldehyde resin as shell material, J. Appl. Polym. Sci. 101 (2006) 1522–1528.
[17] G. Sun, Z. Zhang, Mechanical properties of melamine–formaldehyde microcapsules, J. Microencapsulation 18 (5) (2001) 593–602.
[18] W. Li, X.X. Zhang, X.C. Wang, J.J. Niu, Preparation and characterization of microencapsulated phase change material with low remnant formaldehyde content, Mater. Chem. Phys. 106 (2007) 437–442.
[19] N. Sarier, E. Onder, The manufacture of microencapsulated phase change materials suitable for the design of thermally enhanced fabrics, Thermochim. Acta 452 (2007) 149–160.
[20] G.Y. Fang, H. Li, F. Yang, X. Liu, S.M. Wu, Preparation and characterization of nano-encapsulated *n*-tetradecane as phase change material for thermal energy storage, Chem. Eng. J. 153 (2009) 217–221.
[21] J.P. Wang, X.P. Zhao, H.L. Guo, Preparation of microcapsules containing two-phase core materials, Langmuir 20 (2004) 10845–10850.
[22] Y.B. Cai, Q.F. Wei, F.L. Huang, S.L. Lin, F. Chen, W.D. Gao, Thermal stability, latent heat and flame retardant properties of the thermal energy storage phase change materials based on paraffin/high density polyethylene composites, Renew. Energy 34 (2009) 2117–2123.
[23] P. Liu, Z.X. Su, Thermal stabilities of polystyrene/silica hybrid nanocomposites via microwave-assisted in situ polymerization, Mater. Chem. Phys. 94 (2005) 412–416.
[24] Y.L. Liu, W.L. Wei, K.Y. Hsu, W.H. Ho, Thermal stability of epoxy-silica hybrid materials by thermogravimetric analysis, Thermochim. Acta 412 (2004) 139–147.
[25] A. Sari, A. Karaipekli, Preparation, thermal properties and thermal reliability of palmitic acid/expanded graphite composite as form-stable PCM for thermal energy storage, Sol. Energy Mater. Sol. Cells 93 (2009) 571–576.
[26] G.L. Song, S.D. Ma, G.Y. Tang, Z.S. Yin, X.W. Wang, Preparation and characterization of flame retardant form-stable phase change materials composed by EPDM, paraffin and nano magnesium hydroxide, Energy 35 (2010) 2179–2183.
[27] P. Zhang, Y. Hua, L. Song, H.D. Lua, J. Wang, Q.Q. Liu, Synergistic effect of iron and intumescent flame retardant on shape-stabilized phase change material, Thermochim. Acta 487 (2009) 74–79.